

Fabrication of Co³⁺ and B co-doping BiVO₄ with improved photocatalytic performance for organic degradation

Zhilin Li, Chongyue Jin and Min Wang^a

School of Mechanical Engineering and Automation, Northeastern University, Shenyang 110189, China

Abstract. Co³⁺ and B co-doping BiVO₄ photocatalysts were successfully prepared for organic pollutants degradation through sol-gel and impregnation two-step process. Their structure, surface chemical composition, and optical absorption were characterized. All as-prepared samples consisted of the monoclinic phase. It was found that the Co dopants were existed in the form of Co₃O₄ in B-BiVO₄, thus a p-n heterojunction formed in BiVO₄. The optical absorption results reveal that Co₃O₄ could greatly enhance the absorption and decrease in the band-gap energy of BiVO₄. The 0.5% Co³⁺ doping B-BiVO₄ sample exhibited the highest photocatalytic activity for methyl orange photocatalytic degradation, being approximately 92% of MO degradation rate under 50 min visible light irradiation.

1 Introduction

As one of the non-titania visible-light-driven photocatalysts, BiVO₄ has recently attracted considerable attention, as it is commonly used as a photocatalyst in water splitting and oxidative decomposition of organic pollutants under visible-light irradiation [1-5]. It has been found that the photocatalytic activity of BiVO₄ is determined by its crystal phase. BiVO₄ with a monoclinic scheelite structure can show photocatalytic properties and is commonly used as a photocatalyst in water splitting and oxidative decomposition of organic contaminants under visible light irradiation [6-8]. The photocatalytic activity of pure BiVO₄ still needs improvement due to its high rate of photogenerated electron-hole pair recombination. The introduction of dopant elements causes the formation of charge traps for electrons and/or holes and thus prolongs the recombination time [9].

In the current study, the strategy of Co³⁺ and B co-doping was employed to improve the photocatalytic performance of BiVO₄ photocatalyst. The Co³⁺ doping B-BiVO₄ photocatalysts were successfully prepared for organic pollutants degradation through sol-gel and impregnation two-step process. The effects of Co³⁺ doping on the structure, light absorption ability and photocatalytic performance of B-BiVO₄ were studied in detail.

2 EXPERIMENT

2.1 Photocatalyst preparation

The BiVO₄ and B-BiVO₄ precursors were synthesized

through a sol-gel method as reported in reference [10]. The Co³⁺ and B co-doping BiVO₄ samples were prepared by the impregnation method. The B-BiVO₄ precursor powder (3.0 g) was added to 2 mL of distilled water containing an appropriate amount of Co(NO₃)₂ in a ceramic dish. Water was evaporated at 353 K. The suspension was stirred using a glass rod during evaporation. The resulting powder was collected and calcined in air at 500 °C for 5 h, and then cooled to room temperature to obtain Co³⁺ doping B-BiVO₄ samples, labeled as xCo-B-BiVO₄ nanoparticles. The Co doping concentration (x wt %) was chosen as 0.3, 0.4, 0.5, 0.6, and 0.7, which is the weight percentage of Co(NO₃)₂ to BiVO₄. 0.5Co doping BiVO₄ was prepared with the same impregnation method except that its precursor is pure BiVO₄. For comparison, pure BiVO₄ and B-BiVO₄ were prepared according to reference [10].

2.2 Characterization of photocatalyst

The X-ray diffraction (XRD) spectra of the catalysts were obtained by X-ray diffraction (XRD) with Cu K α radiation (model D/max RA, Rigaku, Japan). The accelerating voltage and the current were 40 kV and 150 mA, respectively. The morphologies of the samples were observed with a field emission scanning electron microscope (SEM, S-3000N, Hitachi, Japan), and the chemical composition of the photocatalysts was determined using an energy dispersive X-ray spectrometer (EDS) attached to the SEM. The binding energies of Bi, V, Co, B, and O were measured at room temperature using an X-ray photoelectron spectroscopy (XPS, VGESCALAB MARK II) using Mg K α radiation. The diffuse reflectance spectra (DRS) were obtained for

^a Min Wang: wangmin@me.neu.edu.cn

the dry-pressed disk samples using a UV-vis spectrophotometer (TU-1901, Puxi, China) equipped with an integrating sphere assembly using BaSO₄ as the reflectance standard. The spectra were recorded in the wavelength range from 230 to 800 nm at 25 ± 1 °C.

2.3 Photocatalytic performance test

The photocatalytic activities of the samples were determined by measuring the degradation of methyl orange (MO) in an aqueous solution under visible light irradiation. In the activity test, a 250 W tungsten halogen lamp with a < 420 nm cutoff filter was used as visible light source. The photo-degradation experiment was performed according to the following process: The photocatalyst (0.01 g) was suspended in 50 mL aqueous solution of methyl orange with the initial concentration of 15 mg/L. The suspension was vigorously stirred with a magnetic stirrer in the dark for 60 minutes prior to illumination to achieve adsorption/desorption equilibrium, as well as in the photoreactor throughout the experiment. At given time intervals, the collected samples were filtered through a 0.45 μm Millipore filter to remove catalyst particles. The filtrate concentration was monitored by recording the absorbance at 464 nm, the maximum absorption wavelength for methyl orange, using a UV-1800 UV-Vis spectrophotometer (Puxi, China).

3 Results and discussion

3.1 XRD analysis

The XRD patterns of as-prepared samples are shown in Fig. 1. All the as-prepared samples exhibited typical peaks of monoclinic BiVO₄ (JCPDS cards No. 75-1866)[2,5]. Although some studies in the literature have reported that Co(NO₃)₂ can be transformed into Co₃O₄ during the calcination process [11], no Co₃O₄ peaks were found in XRD analysis, which might be attributed to the low Co content. Fig. 1 (B) shows the shift of the peaks at approximately 28.8 and 30.5° corresponding to the (121) and (040) planes, respectively. The peaks shift toward the left in the case of B single doping, but our results show a gradual shift toward the right as the Co doping content increased. The right shift suggests that the Co cation was successfully doped into the BiVO₄ and the increased amount of Co dopant in the samples lead to a change in the local crystal structures by a few degrees.

3.2 SEM analysis

The morphology of the synthesized samples was analyzed by SEM. Fig. 2 shows the three typical SEM images of the BiVO₄, B-BiVO₄, and B-0.5Co-BiVO₄ photocatalysts. All three samples displayed a sphere-like morphology, but there is a minor difference in the morphologies and particle shapes of the samples between pure BiVO₄ and B-BiVO₄. After Co doping, the sizes of

some particles decreased, which could cause an increase in the surface area of the sample. The composition of the B-0.5Co-BiVO₄ sample is determined by energy dispersive X-ray spectroscopy (EDX) experiments. As shown in Fig. 2d, we can see the clear signals for Bi, V, O, and Co.

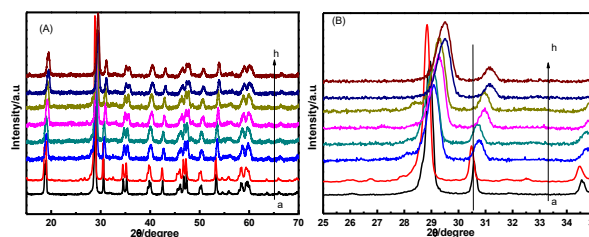


Fig. 1 XRD patterns of different BiVO₄ samples for a. BiVO₄, b. B-BiVO₄, c. 0.5Co-BiVO₄, d. 0.3Co-B-BiVO₄, e. 0.4Co-B-BiVO₄, f. 0.5Co-B-BiVO₄, g. 0.6Co-B-BiVO₄, h. 0.7Co-B-BiVO₄

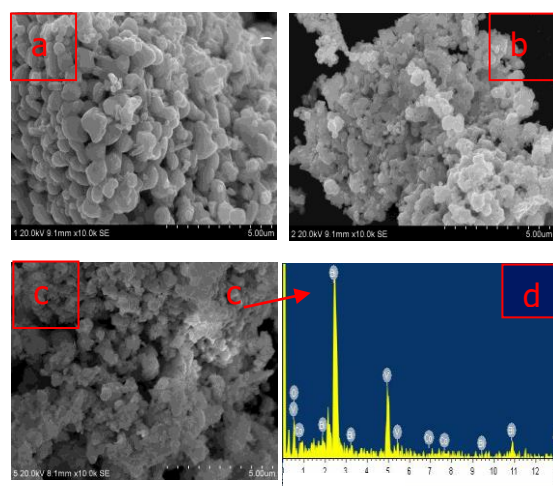


Fig. 2 SEM images of a. pure BiVO₄, b. B-BiVO₄, c. 0.5Co-B-BiVO₄, and d. EDX of 0.5Co-B-BiVO₄

3.3 XPS analysis

The chemical states and chemical compositions of the samples are investigated through XPS. Fig. 3 shows the Co 2p (a), Bi 4f (b), B 1s(c,d), V2p(e), and O1s(f) XPS spectra of the as-prepared samples. The Co 2p high-resolution XPS scan spectrum is shown in Fig. 3 (a). Two peaks at 780.7 and 797.3 eV, which can be assigned to the Co 2p_{3/2} and Co 2p_{1/2}, respectively, were observed. These peaks are very close to those of Co₃O₄ [12], for which corresponding peaks were reported at 780.8 and 797.1 eV.

Fig. 3(b) shows the Bi 4f high-resolution XPS scan spectrum of pure BiVO₄, B-BiVO₄ and 0.3 B-0.5Co-BiVO₄; the binding energies of Bi 4f appear at 159.1~159.5 eV and 164.4 ~165.2 eV for Bi 4f_{7/2} and Bi 4f_{5/2}, respectively, which are characteristic of the Bi³⁺ species [2-7]. The B 1s XPS spectra of the B-doped and B-Co codoped samples are shown in Fig. 3(c) and (d). Each XPS spectrum of B 1s in Fig. 3(c) and (d) exhibits an asymmetric broad peak from 184 to 191 eV, which is a typical characteristic peak for B 1s species. The asymmetric peak was deconvoluted into two components at E_b = 184.2 and 190.8 eV for B-BiVO₄, and

$E_b = 184.3$ and 188.8 eV for B-0.5Co-BiVO₄. The peak at 184.2 and 185.5 eV is assigned to B₄C [13], which showed no photocatalytic activity.

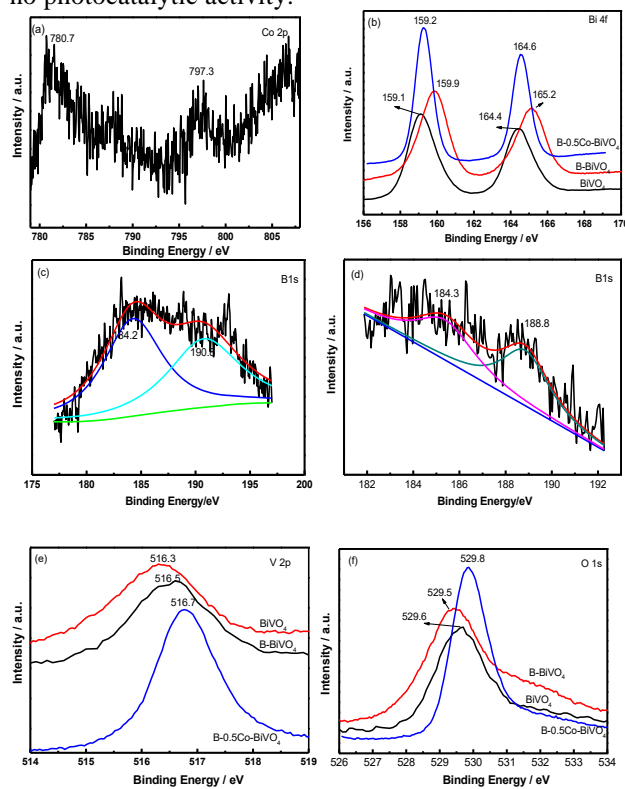


Fig. 3 (a) Co 2p XPS spectra for B-0.5Co-BiVO₄; (b) Bi 4f XPS spectra for BiVO₄, B-BiVO₄, and B-0.5Co-BiVO₄ sample; (c) B 1s XPS spectra for B-BiVO₄, and (d) B 1s XPS spectra for B-0.5Co-BiVO₄ samples; (e) V 2p and (f) O 1s XPS spectra of BiVO₄, B-BiVO₄, and B-0.5Co-BiVO₄ sample

The standard binding energies for B 1s in B₂O₃, H₃BO₃ (B-O bond), and VB₂ (V-B bond) are 193.6 eV [13], 193.0 eV [14], 188.3 eV [15], respectively. It may be concluded that a portion of the B atoms might be doped in the BiVO₄ lattice, replacing the O to form a B-Bi-O bond for this B-BiVO₄ sample. After further doping with Co, the binding energy of B 1s changed to 188.8 eV. This is possibly due to the doping Co ions replacing some Bi ions to form B-Co-O-bonds considering that the standard binding energies for B 1s in CoB is 188.5 eV [12]. However, we can deduce that there is not some CoB phase appearing in the BiVO₄ because the binding energy of Co in 0.5Co-B-BiVO₄ sample is 780.7 eV, as compared with CoB which is approximately 778 eV (as shown in Fig. 3(a)). The XPS results show that both B and Co are successfully doped into the BiVO₄ lattice. Fig. 3 (e) shows the V 2p XPS spectra of pure BiVO₄, B-BiVO₄, and 0.5Co-B-BiVO₄. The V 2p_{3/2} signals have peaks at $E_b = 516.3$ eV for BiVO₄, $E_b = 516.5$ eV for B-BiVO₄, and $E_b = 516.7$ eV for 0.5Co-B-BiVO₄, which correspond the V⁵⁺[7]. The peaks at binding energies of 529.6 eV for pure BiVO₄, 529.6 eV for the B-BiVO₄, and 529.8 eV 0.5Co-B-BiVO₄ correspond to the O 1s, as shown in Fig. 3(f). It is worth noting that the binding energy of O 1s for B-0.5Co-BiVO₄ shifts to higher position (529.8 eV). It is known that the smaller electronegativity of Co (1.88) compared with the Bi (2.02), it led to stronger chemical binding of Co-O bond and increased O 1s binding energy [12].

3.4 UV-Vis DRS analysis

The UV-Vis DRS of the pure BiVO₄, B-BiVO₄, Co-BiVO₄, and B-xCo-BiVO₄ catalysts are shown in Fig. 4. All samples exhibit different absorption spectra in the visible light region. The absorption edge of pure BiVO₄ is determined to be 529 nm. Band gap energy (E_g) can be used to evaluate the optical absorption performance of BiVO₄. The E_g was determined from the equation of $(\alpha/h\nu)^2 = A(h\nu - E_g)^n$, where the A , α , and $h\nu$ represent a constant, absorption coefficient, and incident photon energy, respectively. In the case of direction transition for BiVO₄, the value of n is 1 [6]. The E_g value of BiVO₄ samples can be estimated from a plot of $(\alpha/h\nu)^2$ versus photon energy ($h\nu$), as shown in Fig. 4. The intercept of the tangent to the X-axis is approximately equal to the E_g value. Thus, the E_g can be estimated to be approximately 2.40. For B-BiVO₄, due to the introduction of small amounts of boron, red shift of the absorption spectrum occurred. Some authors proposed that the visible light response was due to the narrowing of the band gap by mixing B 1s and O 2p states [13]. The corresponding band-gap energy for the B-BiVO₄ catalyst is 2.36 eV. The presence of Co₃O₄ results in an increase in the capacity for visible light absorption, which should be attributed to the small band gap of Co₃O₄. Co₃O₄ is a p-type semiconductor with direct transition at 1.45 and 2.07 eV [12], corresponding, respectively, to edges of O²⁻ → Co³⁺ excitation and O²⁻ → Co²⁺ charge transfer. The latter is the basic optical band gap energy for interband transitions. Co₃O₄ has absorption in nearly the entire visible range of the spectrum and induces an extension of the light absorption spectrum of the composite semiconductor even with low cobalt content. Thus, with the increase of Co doping concentration, the absorption is strengthened in the visible region, and the band gap energies decrease. The band gaps of Co-doped and xCo-B-BiVO₄ (x is 0.3, 0.4, 0.5, 0.6, 0.7) are 2.33, 2.31, 2.26, 2.23, 2.21 and 2.11, respectively.

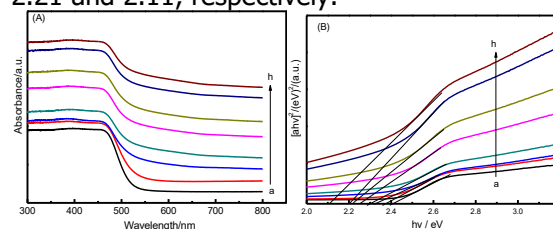


Fig. 4 UV-Vis absorption spectra (A) and $(ah\nu)^2 - h\nu$ curves (B) of some samples- a. BiVO₄, b. B-BiVO₄, c. 0.5Co-BiVO₄, d. B-0.3Co-BiVO₄, e. B-0.4Co-BiVO₄, f. B-0.5Co-BiVO₄, g. B-0.6Co-BiVO₄, h. B-0.7Co-BiVO₄

3.5 Photocatalytic performance

The photocatalytic degradation of MO dye on the as

prepared BiVO_4 catalysts was carried out under visible-light irradiation. The results are shown in Fig. 5. It shows that only a small amount of MO could be degraded through either direct photolysis in the absence of catalyst or adsorption in the dark. The evidence indicates that the pure BiVO_4 a catalysts exhibited low visible light photocatalytic efficiency for the degradation of MO within 50 min irradiation. Compared with pure BiVO_4 , B- and Co- single doped BiVO_4 can enhance the photocatalytic activity to some degree. However, it can be obviously observed that B-Co codoping can increase BiVO_4 photocatalytic activity effectively. The MO photocatalytic degradation rate for B-Co codoped BiVO_4 increases with Co doping content when the doping Co is lower than 0.5%, but decreases when the amount of Co is higher than 0.5%. The degradation rate of MO can be up to 92% in 50 min. So the optimal mole percentage of Co doping in B-Co codoping BiVO_4 , is 0.5%. These results confirmed that Co and B elements exhibited a synergetic effect on the improvement of photocatalytic activity efficiency. Moreover, as displayed in Fig. 5(B), the photocatalytic degradation of MO solution fitted well with the pre-first-order kinetics according to the Langmuir-Hinshelwood (L-H) model within 50 min.

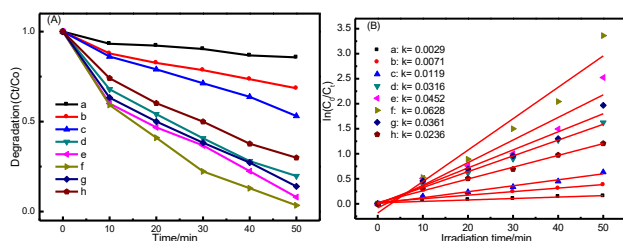


Fig. 5 (A) MO degradation under visible light illumination for 50 min in the presence of B- BiVO_4 with various nickel doping, pure BiVO_4 and without photocatalyst; (B) $\ln(C_0/C_t)$ versus time for B- BiVO_4 doping concentrations of a. BiVO_4 , b. B- BiVO_4 , c. 0.5Co- BiVO_4 , d. B-0.3Co- BiVO_4 e. B-0.4Co- BiVO_4 , f. B-0.5Co- BiVO_4 , g. B-0.6Co- BiVO_4 , h. B-0.7Co- BiVO_4

Based on the above analysis, the scheme that the as prepared Co^{3+} and B codoped BiVO_4 catalysts exhibited higher photocatalytic efficiency can be explained as following scheme (Fig. 6): in the case of Co^{3+} and B codoped BiVO_4 , on the one hand, the impurity energy levels are introduced above the valence band due to B dopants, thus causing the absorption edge to shift into the visible region. The impurity levels create another possible transition route for excited electrons during visible light irradiation, which electrons are promoted from the B1s level to the conduction band of BiVO_4 . On the other hand, because the Co_3O_4 [23] is a p-type semiconductor and BiVO_4 is an n-type material [1], a p-n heterojunction formed at the interface of the two materials in the composite photocatalysts. The photoinduced electrons on the BiVO_4 particle surface can easily migrate to Co_3O_4 via interfaces; similarly, photoinduced holes on the Co_3O_4 surface can transfer to BiVO_4 owing to the different valence band edge potentials. As a result, a larger amount of electrons on the Co_3O_4 surface and holes on the BiVO_4 surface can participate in photocatalytic

reactions to directly or indirectly decompose MO, thus enhancing the photocatalysis efficiency.

However, more Co_3O_4 can also act as recombination centers for the electrons and holes. Therefore, an appropriate amount of the doped Co in B- BiVO_4 catalysts is necessary so that the recombination of photogenerated electrons and holes can be suppressed effectively. It is interesting to note that the photocatalytic activities of B and Co_3O_4 codoped BiVO_4 catalysts enhance with the increase in Co doping content up to 0.5% and then decrease. A similar result was also reported by Zhang et al. [30]. It is hypothesized that high Co_3O_4 content is harmful to the photocatalytic activity because of the excess coverage of active sites on the BiVO_4 surface by Co_3O_4 particles and can also act as recombination centers for the electrons and holes [16].

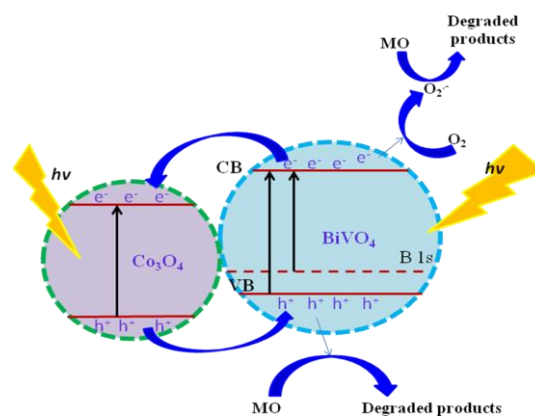


Fig.6 Proposed degradation scheme of organic pollutants by B-Co- BiVO_4 under visible light irradiation.

4 Conclusions

Co^{3+} and B codoped BiVO_4 catalysts were successfully prepared through a sol-gel and impregnation two-step process. Compared with the pure BiVO_4 , B-, Co- single-doped BiVO_4 , the Co^{3+} and B codoped BiVO_4 exhibits higher photoactivity under visible light. These samples show higher photocatalytic activity for methyl orange photocatalytic degradation, and the highest degradation rate for B-0.5Co- BiVO_4 can reach to be approximately 92% under visible light irradiation in 50 min. The B dopants led to impurity energy levels above the valence band and a p-n heterojunction formed due to Co_3O_4 being a p-type semiconductor and BiVO_4 an n-type. Codoping can narrow the band gap. The synergetic effects of B and Co_3O_4 may efficiently promote the separation of photogenerated holes and electrons and are the main reasons for the high photodegradation rate of dye pollutants under visible light irradiation.

References

1. F. Chen, Q. Yang, X.M. Li, G.M. Zeng, D.B. Wang, C.G. Niu, Appl. Catal. B: Environ. 200 (2017) 330-342.

2. R.Z. Sun, Q.M. Shi, M. Zhang, L.H. Xie, J.S. Chen, X.M. Yang, M.X. Chen, W.R. Zhao, *J. Alloys Compd.* 714 (2017) 619-626.
3. M. Wang, Y.S. Che, C. Niu, M.Y. Dang, D. Dong, *J. Hazard. Mater.* 262 (2013) 447-455.
4. H.J. Kong, H.W. Da, J. Kim, S.I. Woo, *Chem. Mater.* 28 (2016) 1318-1324.
5. Z.B. Xiang, Y Wang, D. Zhang, P. Ju, *J. Ind. Eng. Chem.* 40 (2016) 83-92.
6. X. Chang, T. Wang, P. Zhang, J.J Zhang, A. Li, J. L. Gong. *J. Am. Chem. Soc.* 137 (2015) 8356-8359.
7. S.S. Xue, H.B. He, Z. Wu, C.L. Yu, Q.Z. Fan, G.M. Peng, K. Yang, *J. Alloys Compd.* 694 (2017) 989-997.
8. M. Wang, P. Y. Guo, T. Y. Chai, Y. H. Xie, J. Han, M. Y. You, Y. Z. Wang , T. Zhu, *J. Alloys Compd.* 691(2017)8-14.
9. L. Yan , W. Zhao, Z. Liu, *Dalton Trans*, 45 (2016) 11346-11352.
10. M. Wang, H. Y. Zheng, Q. Liu, C. Niu, Y. S. Che, M. Y. Dang, *Spectrochim. Acta, Part A*, 114(2013) 74-79
11. B. Zhou, X. Zhao, H.J. Liu, J.H. Qu, C.P. Huang, *Sep. Purif. Technol.* 77 (2011) 275-282.
12. C. L. Yu, K. Yang, J. C. Yu, F. F. Cao, X. Li , X. C. Zhou. *J. Alloys Compd.* 509 (2011) 4547-4552.
13. H. J. Long, Q. J. Meng, J. Yuan, W. S. Yang, Y.A. Cao, *Acta. Chim. Sinica.*, 66 (2008) 657-661.
14. C. D. Wagner, W. M. Riggs, L.E. Davis, J.F. Moulder, in:G.E. Muilenberg(Ed.). *Handbook of X-Ray Photoelectron Spectroscopy*, Perkin-Elmer Co., Minnesota, 1979.
15. F. Y. Wei, L.S. Ni, *Chin. J Catal.*, 28(2007) 905-909.
16. C. L. Yu, K. Yang, J. C. Yu, F. F. Cao, X. Li , X. C. Zhou. *J. Alloys Compd.* 509 (2011) 4547-4552.